ANTIOXIDANTS & REDOX SIGNALING
Volume 13, Number 6, 2010

DOI: 10.1089/ars.2009.3018

ORIGINAL RESEARCH COMMUNICATION

Neuroprotective Mechanism of Mitochondrial Ferritin on 6-Hydroxydopamine–Induced Dopaminergic Cell Damage: Implication for Neuroprotection in Parkinson's Disease

Zhen-Hua Shi,[1,2,*] Guangjun Nie,[3,*] Xiang-Lin Duan,[1] Tracey Rouault,[4] Wen-Shuang Wu,[1] Bo Ning,[3] Nan Zhang,[1] Yan-Zhong Chang,[1] and Bao-Lu Zhao[2]

Abstract

Neuronal iron homeostasis disruption and oxidative stress are closely related to the pathogenesis of Parkinson's disease (PD). Adult iron-regulatory protein 2 knockout (*Ireb2*$^{-/-}$) mice develop iron accumulation in white matter tracts and nuclei in different brain area and display severe neurodegeneration in Purkinje cells of the cerebrum. Mitochondrial ferritin (MtFt), a newly discovered ferritin, specifically expresses in high energy–consuming cells, including neurons of brain and spinal cord. Interestingly, the decreased expression of MtFt in cerebrum, but not in striatum, matches the differential neurodegeneration pattern in these *Ireb2*$^{-/-}$ mice. To explore its effect on neurodegeneration, the effects of MtFt expression on 6-hydrodopamine (6-OHDA)-induced neuronal damage was examined. The overexpression of MtFt led to a cytosolic iron deficiency in the neuronal cells and significantly prevented the alteration of iron redistribution induced by 6-OHDA. Importantly, MtFt strongly inhibited mitochondrial damage, decreased production of the reactive oxygen species and lipid peroxidation, and dramatically rescued apoptosis by regulating Bcl-2, Bax and caspase-3 pathways. In conclusion, this study demonstrates that MtFt plays an important role in preventing neuronal damage in an 6-OHDA–induced parkinsonian phenotype by maintaining iron homeostasis. Regulation of MtFt expression in neuronal cells may provide a new neuroprotective strategy for PD. *Antioxid. Redox Signal.* 13, 783–796.

Introduction

PARKINSON'S DISEASE (PD) is a common neurodegenerative disease characterized by the loss of dopaminergic neurons in the substantial nigra (SN) and the formation of filamentous intraneuronal inclusions, with clinical symptoms of rigidity, resting tremor, and bradykinesia (34). Although PD etiology remains mysterious, it has been proposed that disruption of iron homeostasis, dysfunctions of mitochondria, and oxidative stress play key roles in the pathogenesis of PD (19, 27, 51, 52). Analysis of postmortem PD SN reveals increased nonheme iron in the SN and nigra (12, 40, 52). If iron is causally involved in the cellular degeneration associated with toxin-induced parkinsonism, it would be expected that antioxidant supplements and iron chelation by iron-storage protein or blood–brain barrier (BBB)-permeable chelators might protect from neuronal cell damage in PD (18, 51). A recent report demonstrated that both transgenic expression of H-ferritin and pharmacologic iron chelation prevent MPTP-induced neurotoxicity *in vivo* (24). However, a missing role for ferritins in the pathophysiologic context of various neurodegenerative diseases still exists.

6-Hydroxydopamine (6-OHDA) is a neurotoxin that causes selective death in catecholamine-containing neurons. As a reactive oxidative species (ROS)-producing agent, this compound has been shown to generate hydrogen peroxide, superoxide radical, and hydroxyl radical (9, 15, 41), which are involved in the PD pathogenesis process. Several lines of evidence also showed that quinine derived from 6-OHDA autooxidation also exerts neuronal toxicity, probably through ER stress (31, 37, 48). Neuroblastoma SH-SY5Y cells treated with 6-OHDA are widely used as a valuable cell model of

[1]Laboratory of Molecular Iron Metabolism, College of Life Science, Hebei Normal University, Shijiazhuang, Hebei Province, China.
[2]State Key Laboratory of Brain and Cognitive Science, Institute of Biophysics, Academia Sinica, Beijing, China.
[3]CAS Key Laboratory for Biological Effects of Nanomaterials & Nanosafety, National Center for Nanoscience and Technology of China, Beijing, China.
[4]Molecular Medicine Program, National Institute of Child Health and Human Development, National Institutes of Health, Bethesda, Maryland.
*These authors contributed equally to this work.

dopaminergic neuronal cell death to mimic the pathophysiologic degeneration (17). They also have been used to induce degeneration of the nigrostriatal dopaminergic neurons in animal models of PD (18). 6-OHDA, as a neurotoxin, may cause iron release from cytosolic ferritin (22). These released irons may react with endogenous hydrogen peroxide by Fenton reaction to produce highly toxic hydroxyl free radicals and result in cell death in PD.

Iron-regulatory proteins (IRPs, including IRP1 and IRP2) are ubiquitously expressed regulatory proteins that have a central role in mammalian iron metabolism. Adult IRP2 knockout mice (*Ireb2*$^{-/-}$ mice) accumulate iron in many regions of the brain. Numerous severe Purkinje cells degenerations were observed in cerebellum particularly (25, 39).

Cytosolic ferritins (H and L ferritins) are ubiquitous proteins with a defined function of sequestration and storage of iron as a safe and accessible reserve of iron in cytoplasm (2, 3, 44). Because excess free iron might generate damaging ROS as byproducts during mitochondrial electron transport, ferritins, under the influence of iron and oxygen metabolism, exert cellular protective roles against iron-mediated free radical damage (2, 3, 13). Mitochondrial ferritin (MtFt) is a recently identified H-ferritin–like protein (26) that has been shown to modulate cellular iron metabolism dramatically (10, 26, 30). Its physiologic expression is restricted to mitochondria of testes, the central nervous system, and other high oxygen-consumption tissues (38). Although overexpression of MtFt modulates intracellular iron homeostasis (10, 26, 30), no study has explored the functions of MtFt on neuronal cell iron metabolism and the possible roles of neurodegeneration, such as in PD.

In this study, we first confirmed the endogenous expression of MtFt in the cerebellum and striatum of mice and found that MtFt expression decreased significantly in the cerebellum, but not in the striatum of *Ireb2*$^{-/-}$ mice compared with their wild-type counterparts. This differential expression pattern of MtFt matches well with the severe neurodegeneration observed in the cerebellum of *Ireb2*$^{-/-}$ mice. Based on these observations, we hypothesized that downregulation of MtFt in the cerebellum may be involved in neuronal cell death in *Ireb2*$^{-/-}$ mice, and MtFt plays important roles in neurodegeneration in PD and PD-like syndromes. To explore this hypothesis, we transfected the mouse mitochondrial ferritin gene into SH-SY5Y cells and established a stable-transfected cell line, MtFt-SY5Y, to investigate the function of MtFt on a PD cell model induced by 6-OHDA. Our current study demonstrates that MtFt can dramatically affect neuronal cell iron metabolism and significantly prevent neuronal cell damage induced by 6-OHDA. The current observations, together with the specific distribution in high oxygen-consumption tissues and cells, suggest that the regulation of ferritin expression in neuronal mitochondria may provide a new neuroprotective strategy for neurodegenerative diseases, such as in PD.

Materials and Methods

Materials

Dulbecco's modified Eagle's medium (DMEM), fetal calf serum, 4-(2-hydroxyethyl) − 1-piperazineethanesulfonic acid (HEPES) were purchased from Gibco BRL (Grand Island, NY). 6-OHDA, 2′,7′-dichlorofluorescein diacetate (DCF-DA), rhodamine 123 (Rh123), annexin V, propidium iodide (PI), Hoechst 33258, 3-(4,5-dimethylthiazol-2-yl)-2,5-diphenyltetrazolium-bromide (MTT), calcein-AM, Fluo-3-AM, decylubiqinone, NADH, penicillin, and streptomycin were purchased from Sigma (St. Louis, MO). Lipofectamine 2000 was purchased from Invitrogen (San Diego, CA). The plasmid of mouse mitochondrial ferritin and blank plasmid pcDNA3.1(-) were described in previous articles (30). Anti-HA, β-actin, Bcl-2, Bax, TfR, ferritin, and cytochrome *c* antibodies were purchased from Santa Cruz Biotechnology (Santa Cruz, CA). The antibodies against DMT1 (+IRE), DMT1 (-IRE), and ferroportin are from Alpha Diagnostic International (San Antonio, TX). The anti-MtFt antibody was a gift from Professor Sonia Levi.

Animals

Wild-type and *Ireb2*$^{-/-}$ mice (lack of IRP2 protein) were housed in stainless steel rust-free cages at 22 to 24°C, 45% to 55% relative humidity in NIH. All animals were provided free access to food and distilled water. The experimental animals were 14 months old. All experimental procedures were performed according to U.S.A. animal safety regulations.

Generation of stable MtFt-expressing cell line and 6-OHDA treatment

The plasmid of mouse MtFt-pcDNA3.1(-) and the empty plasmid of pcDNA3.1(-) were transfected into SH-SY5Y cells with Lipofectamine 2000, according to the manufacturer's instructions. Stable transfectants were selected in medium containing 1,000 μg/ml G418. Representative clones were isolated for further characterization. The cells were maintained in DMEM supplemented with heat-inactivated fetal calf serum (10%, vol/vol), glucose (4.5 mg/ml), penicillin (100 U/ml), and streptomycin (100 μg/ml) in humidified 5%CO_2/95% air at 37°C. 6-OHDA was dissolved in PBS with 0.1% vitamin C. The stock solution of 6-OHDA was prepared and stored at −20°C in the dark.

RT–PCR

Total RNA was extracted from cells with *TRIzol* reagent (Invitrogen); 2 mg of total RNA was reverse transcribed into cDNA by using the SuperScript First-Strand Synthesis System (Invitrogen). The PCR-reaction solution was performed according to the following parameters: 94°C denaturation for 4 min, 94°C for 45 s, 57°C for 30 s, and 72°C for 40 s for 32 cycles, followed by 72°C extension for 7 min with TaKaRa Ex Taq Hot Start Version (Takara, Japan) in a Mastercycler ep Realplex 4 Thermor Cycler (Eppendorf). The PCR reaction was electrophoresed on a 2% agarose gel. The primer sequences used for the PCR reaction were as follows: Human MtFt (192bp) sense H-MtFt-F: GCTCTATGCGTCCTACGTG TACTTGT, antisense H-MtFt-R: TCCTGTTCCGGCTTCTTG AT; mouse MtFt (102bp) sense QMtFt1-F: AGCACATCAG CTCTGCACTG, antisense QMtFt1-R: AGGCCAGTAGGGG ACCTAAA.

Assessment of Cell Viability

Cell viability was measured with MTT assay according to the literature (29). In brief, the exponentially growing SH-SY5Y cells, MtFt-transfected cells (MtFt-SY5Y), and vector pcDNA3.1-transfected cells (Vector-SY5Y) were harvested with 0.25% trypsin-0.02% EDTA and then plated at a density of 10^4/well in 96-well plates. After overnight incubation, the

medium was removed and replaced with fresh medium with or without 100 μM 6-OHDA for 24 h. Cell viability was determined by adding MTT (500 μg/ml) to each well, and the mixture was incubated for another 4 h at 37°C. After the medium was removed, cells were lysed with DMSO. The absorbance at 595 nm was measured with a Bio-Rad model 3550 microplate reader (Richmond, CA). The samples were measured in eight replicates, and each experiment was repeated three times.

Morphologic changes

The cells were fixed with Carnoy's fixative buffer containing methanol and glacial acetic acid (3:1, vol/vol) and incubated with Hoechst 33258 (3 μg/ml) for 30 min. The nuclear morphology was observed with fluorescence microscopy (Olympus, kx14e). Nuclear-size reducing, chromatin condensation, intense fluorescence, and nuclear fragmentation were considered apoptosis.

Detection of cell apoptosis by annexin V/propidium iodide staining

6-OHDA-induced apoptosis in SH-SY5Y, MtFt-SY5Y, and Vector-SY5Y cells was measured by annexin V/propidium iodide (PI) staining, followed by FACS measurement of their emissions, as described in the literature (29).

Measurement of release of cytochrome c

The release of cytochrome *c* was measured with Western blotting with extracts of cytosolic fractions. Cytochrome *c* immunofluorescence was measured according to the literature (8), with minor modifications. After treatment with 100 μM 6-OHDA for 24 h, the cells were washed twice in ice-cold PBS. After treatment with 4% polyoxymethylene overnight at 4°C, the cells were washed with prechilled absolute methanol for 5 min, blocked with 5% sheep blood serum for 1 h, and then treated with anti-cytochrome *c* antibody for overnight at 4°C. After washing 3 times, the cells were treated with sheep anti-mouse IgG/FITC for 1 h at 37°C. The release of cytochrome *c* was observed under a fluorescence microscopy (Olympus, kx14e).

Measurement of intracellular ROS

The level of intracellular ROS was quantified by measuring the fluorescence of DCF-DA, according to Guo *et al.* (17). After treatment with or without 100 μM 6-OHDA for 24 h, the cells were collected and washed 3 times with 1×PBS, followed by incubation with 5 μM DCF-DA for 45 min at 37°C in the dark. Then the cells were washed 3 times with 1×PBS and resuspended in BSS buffer containing 130 mM NaCl, 5.4 mM KCl, 0.8 mM $MgCl_2$, 1.8 mM $CaCl_2$, 15 mM glucose, and 5 mM HEPES, pH 7.4. The relative levels of fluorescence were quantified by fluorescence spectrophotometer (Hitachi F-4500, Tokyo, Japan; 485-nm excitation and 535-nm emission), and the data were expressed as a percentage of the fluorescence relative to the fluorescence of the control cells.

Measurement of thiobarbituric acid–reacted substances

The levels of lipid peroxidation were measured by determining TBARS according to Zhang *et al.* (53). Cells were collected and lysed on ice for 20 min by lysis buffer (50 mM Tris–HCl, 150 mM NaCl, and 1% Triton X-100). The samples were mixed with 1 ml of 0.8% (wt/vol) trichloroacetic acid and 0.8 ml double-distilled water. After vortexing, the samples were incubated for 60 min in boiling water, and TBARS were extracted with 3 ml of *n*-butanol. After centrifugation at 4,400 *g* for 10 min, the absorption of the butanol layer was measured at 532 nm. 1,1,3,3-Tetraethoxypropane (TMP) served as MDA standard. TBARS levels were expressed as the ratio of the values of treated samples to the control.

Measurement of mitochondrial membrane potential

The change in mitochondria membrane potential was assayed by measuring the retention of rhodamine 123 (Rh123). In brief, after treatment with or without 6-OHDA, the medium was removed and replaced with fresh nonserum medium containing 10 μM Rh123 for 15 min at 37°C in the dark. Then the cells were washed 3 times with 1×PBS. The Rh123-specific fluorescence intensity was monitored at an excitation wavelength of 490 nm and an emission wavelength of 515 nm by using a Hitachi F-4500 fluorescence spectrophotometer (Hitachi, Tokyo, Japan). The data were expressed as a percentage of the fluorescence in samples relative to the fluorescence in the control cells.

Assessment of complex I activity of mitochondrial respiratory chain

The complex I activity was measured according to Janssen (23). In brief, 960-μl reaction solution (containing 25 mM potassium phosphate, 3.5 g/L BSA, 60 μM DCIP, 70 μM decylubiquinone, 1.0 μM antimycin-A, pH 7.8) was mixed with 20 μl mitochondrial fraction from cells at 37°C. After 3 min, 20 μl of 10 mM NADH (dissolved in dimethyl sulfoxide) was added, and the absorbance at 600 nm was measured at 30-s intervals for 4 min at 37°C. After 4 min, 1.0 μl rotenone (1 mM in dimethyl sulfoxide) was added, and the absorbance was measured again at 30-s intervals for 4 min. The complex I activity was expressed as units per milligram protein (1 U of complex I activity is equal to reduction of 1 μM DCIP per min).

Measurement of the levels of intracellular labile iron pool

The LIP levels were measured according to the literature (14), with minor modifications. In brief, after treatment with or without 6-OHDA, the cells were harvested, washed, and resuspended in a medium containing 140 mM NaCl, 5 mM KCl, 1 mM $MgCl_2$, 5.6 mM glucose, 1.5 mM $CaCl_2$, and 20 mM Hepes (pH 7.4). Calcein-AM was added to a final concentration of 0.25 μM. The reaction mixture was subsequently incubated for 30 min at 37°C. After washing 3 times, the cells were resuspended in the medium and transferred to a cuvette. The fluorescence intensity of calcein-AM was quantified by a fluorescence spectrophotometer (Hitachi F-4500), at an excitation wavelength of 485 nm and an emission wavelength of 520 nm. When the baseline was stable, 100 μM salicylaldehyde isonicotinoyl hydrazone (SIH) (final concentration, 100 μM) was added, and the increase of the fluorescence reflected the levels of calcein-bound iron.

Measurement of intracellular calcium concentration

The concentration of intracellular Ca^{2+} was measured with Fluo-3-AM according to the method of Zhang *et al.* (53) with minor modifications. Cells were harvested, washed, and resuspended in the medium containing 140 m*M* NaCl, 5 m*M* KCl, 1 m*M* $MgCl_2$, 5.6 m*M* glucose, 1.5 m*M* $CaCl_2$, and 20 m*M* Hepes (pH 7.4), and then Fluo-3-AM (5 m*M*) was added. The reaction mixture was subsequently incubated for 30 min at 37°C. After washing 3 times, the cells were resuspended in the medium and transferred to a fluorometer cuvette. The fluorescence intensity of Fluo-3 was quantified by a fluorescence spectrophotometer (Hitachi F-4500), at an excitation wavelength of 490 nm and an emission wavelength of 526 nm. The intracellular calcium concentration ($[Ca^{2+}]i$) was calculated from the Fluo-3 fluorescence intensity according to the literature (53).

Western blotting

The 40 μg protein of each sample was loaded in SDS-PAGE, separated on gels (10% for MtFt, Bcl-2, and Bax; 8% for DMT1(+IRE), DMT1(-IRE), and ferroportin; 6% for TfR), and then transferred to nitrocellulose membranes. Blots were blocked in blocking buffer containing 5% fat-free milk, 0.1% Tween 20 in 0.1 *M* TBS, and incubated with primary antibody overnight with constant agitation at 4°C. After washing 4 times, the membranes were incubated with the second antibody for 1 h at room temperature, with constant agitation, and then washed and reacted with the chemiluminescent substrate (Pierce Biotechnology, Rockford IL), and exposed to Kodak-XAR film. The film was digitized and analyzed with an NIH imaging software.

Statistical analysis

All experiments were performed at least in triplicate. One-way ANOVA was used to estimate overall significance, followed by *post hoc* Tukey tests corrected for multiple comparisons. Data are presented as mean ± SD. A probability level of 95% ($p < 0.05$) is considered significant.

Results

Endogenous expression pattern of MtFt in the brain of wild-type and *Ireb2*$^{-/-}$ mice

Although it has been shown that MtFt expression is restricted mainly to tissues with high metabolic activity and oxygen consumption, such as testis, brain, and spinal cord (38), the roles of this protein are largely unknown. Targeted deletion of the IRP2 causes misregulation of iron metabolism and PD-like neurodegeneration in adult mice (25). In the cerebellum of *Ireb2*$^{-/-}$ animals, the Purkinje cell loss is prominent (25). It has been speculated that the MtFt expression pattern in *Ireb2*$^{-/-}$ mice brain may be altered, and the possible changes of MtFt expression may emphasize the neurologic roles of this protein.

We then tested the endogenous expression of MtFt in the cerebellum and striatum of wild-type and *Ireb2*$^{-/-}$ mice. Interestingly, we found a significant decrease of MtFt levels in the cerebellum but not in the striatum of *Ireb2*$^{-/-}$ mice compared with their wild-type counterparts, as shown in Fig. 1A and B. As controls, the levels of actin and mitochondrial protein cytochrome *c* were not changed (Fig. 1A and B). The differential expression pattern of MtFt in the brains of *Ireb2*$^{-/-}$ animals may suggest that the protein is involved in the neurodegenerative process of the Purkinje cell observed in *Ireb2*$^{-/-}$ mice. Aging-related changes of MtFt-expression changes were also been observed. MtFt levels increased gradually with age, reaching the highest level at postnatal 12 weeks in cortex and hippocampus and 44 weeks in striatum, followed by a decrease in aging animals (data not shown). Because cytosolic ferritins are the major cellular protective proteins against iron-mediated oxidative stress, the cell type–specific expression pattern and altered expression with the aging process and in *Ireb2*$^{-/-}$ animals may suggest that the new types of ferritins may play an important role in neuroprotection.

MtFt expression significantly rescues cell death after 6-OHDA treatment

To investigate the possible roles of MtFt in neuroprotection, stably transfected MtFt-SY5Y cells were screened and established. MtFt protein expression was analyzed with Western blotting by using anti-HA tag antibody. As shown in Fig. 1C, a representative clone was selected and used for further characterization. In agreement with previous reports (30), an MtFt protein band exists with an apparent molecular mass of 22 kDa on SDS-PAGE; no such band was detected in SH-SY5Y and vector-transfected cells (Fig. 1C). No significant changes of MtFt expression were noted in 100 μM 6-OHDA–treated MtFt-SY5Y cells for 24 h, as shown in Fig. 1D. The endogenous expression of human MtFt in SH-SH5Y cells is low and not comparable to the levels of overexpressed mouse MtFt in SH-SY5Y cells by RT-PCR measurement (Fig. 1Ei and Eii).

Previously, our studies and those of others have shown that 6-OHDA can decrease the viability of SH-SY5Y in a dose- and time-dependent manner (17, 42). A remarkable decrease in the viability of SH-SY5Y and Vector-SY5Y cells ($\sim$60%; $p < 0.01$, compared with the control groups, respectively) was observed under the treatment of 100 μM 6-OHDA for 24 h (Fig. 2A). However, the viability of MtFt-SY5Y cells decreased >10%, without a significant difference compared with the control groups. These results show that overexpression of MtFt prevents the decrease in cell viability under the 6-OHDA treatment.

Further to study the neuroprotective roles of MtFt, the effects of MtFt on apoptosis were measured with different techniques. First, the levels of apoptosis induced by 6-OHDA treatment were quantified by using annexin V and PI staining, followed by cell flow-cytometry measurement. Figure 2B shows that MtFt has a dramatic antiapoptotic role against the neurotoxin 6-OHDA-induced cell damage. After treatment with 100 μM 6-OHDA for 24 h, the ratio of apoptotic annexin-positive MtFt-SY5Y cells increased from 3.61% to 9.04%; however, the ratios of apoptotic annexin-positive Vector-SY5Y cells increased from 8.29% to 41.26% ($p < 0.01$) (Fig. 2Bi and 2Bii). Second, MtFt expression also markedly prevented the morphologic changes induced by 6-OHDA treatment. As shown in Fig. 2C, the majority of cells in the control groups had normal nuclei staining patterns with the membrane-permeable DNA-binding dye Hoechst 33258. Exposure to 100 μM 6-OHDA for 24 h led to typical apoptosis morphology (condensed chromatin and bright staining) in SH-SY5Y and Vector-SY5Y cells, but not in MtFt-SY5Y cells (Fig. 2C).

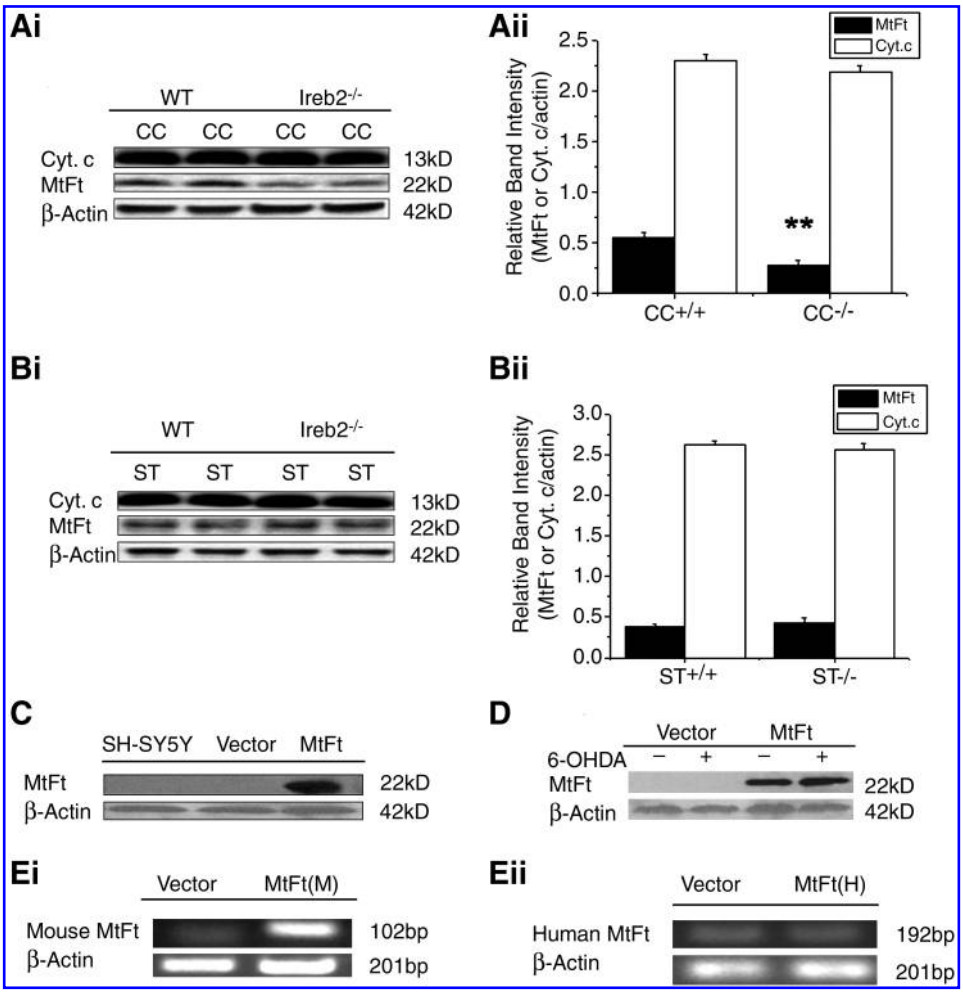

FIG. 1. The endogenous expression of MtFt in the cerebellum and striatum of wild-type (WT) and *Ireb2*$^{-/-}$ mice and the overexpression of mouse MtFt in SH-SY5Y cells. Cerebellum and striatum extracts were analyzed with Western blotting by using anti-MtFt, anti-cytochrome *c*, and *β*-actin antibodies (**Ai**) and (**Bi**). Relative band intensities of MtFt were expressed as the ratio of MtFt to *β*-actin (**Aii**) and (**Bii**) (mean ± SD; $^{**}p < 0.01$ vs. wild-type controls). CC and ST represent cerebellum and striatum, respectively. Overexpression of MtFt in the stably transfected SH-SY5Y cells was detected with Western blotting by using an anti-HA antibody (**C**). No effects of 6-OHDA treatment on the expression of MtFt were detected by Western blotting with an anti-HA antibody (**D**). RT-PCR measurement of overexpressed mouse MtFt messages (**Ei**) and endogenous human MtFt messages (**Eii**).

MtFt expression diminishes the increase in the levels of intracellular ROS, TBARS, and $[Ca^{2+}]_i$ induced by 6-OHDA treatment

Our previous study showed that 6-OHDA treatment increased ROS production in SH-SY5Y cells, resulting in decreases in cell viability and increases in apoptosis (17). In the current study, it was found that 6-OHDA treatment led to a slight increase in intracellular ROS production (18% ± 1.94%) in the MtFt-SY5Y cells, but a significant increase in the levels of ROS in the SH-SY5Y (90% ± 5.86%) and in the Vector-SY5Y (91% ± 4.44%) cells compared with the control groups without 6-OHDA treatment (as shown in Fig. 3A). Therefore, MtFt overexpression significantly decreases the intracellular ROS production induced by 6-OHDA.

Excess ROS production may cause oxidative damage of the cell membrane, proteins, and even DNA. As shown in Fig. 3B, 6-OHDA treatment caused 30% ± 6.14% increase in TBARS formation in Vector-SY5Y cells ($p < 0.05$); however, in the MtFt-SY5Y cells, no significant difference was found compared with the control groups. The results indicate that the expression of MtFt inhibits 6-OHDA–induced lipid peroxidation in the cells.

Elevated ROS and lipid peroxidation production promotes overload of intracellular calcium and consequently leads to apoptosis (53). As shown in Fig. 3C, 6-OHDA treatment led to ~200% ($p < 0.01$) increase in intracellular calcium levels in SH-SY5Y and Vector-SY5Y cells; conversely, in the MtFt-SY5Y cells, significantly lower levels of calcium increase was observed (50% increase, compared with the control groups), indicating that expression of MtFt largely prevents 6-OHDA–induced calcium overload in the cells.

MtFt expression attenuates 6-OHDA-induced decreases in mitochondrial membrane potential and complex I activity and prevents cytochrome c release

The state of mitochondrial membrane potential reflects the metabolic activity of mitochondria and has a close relation

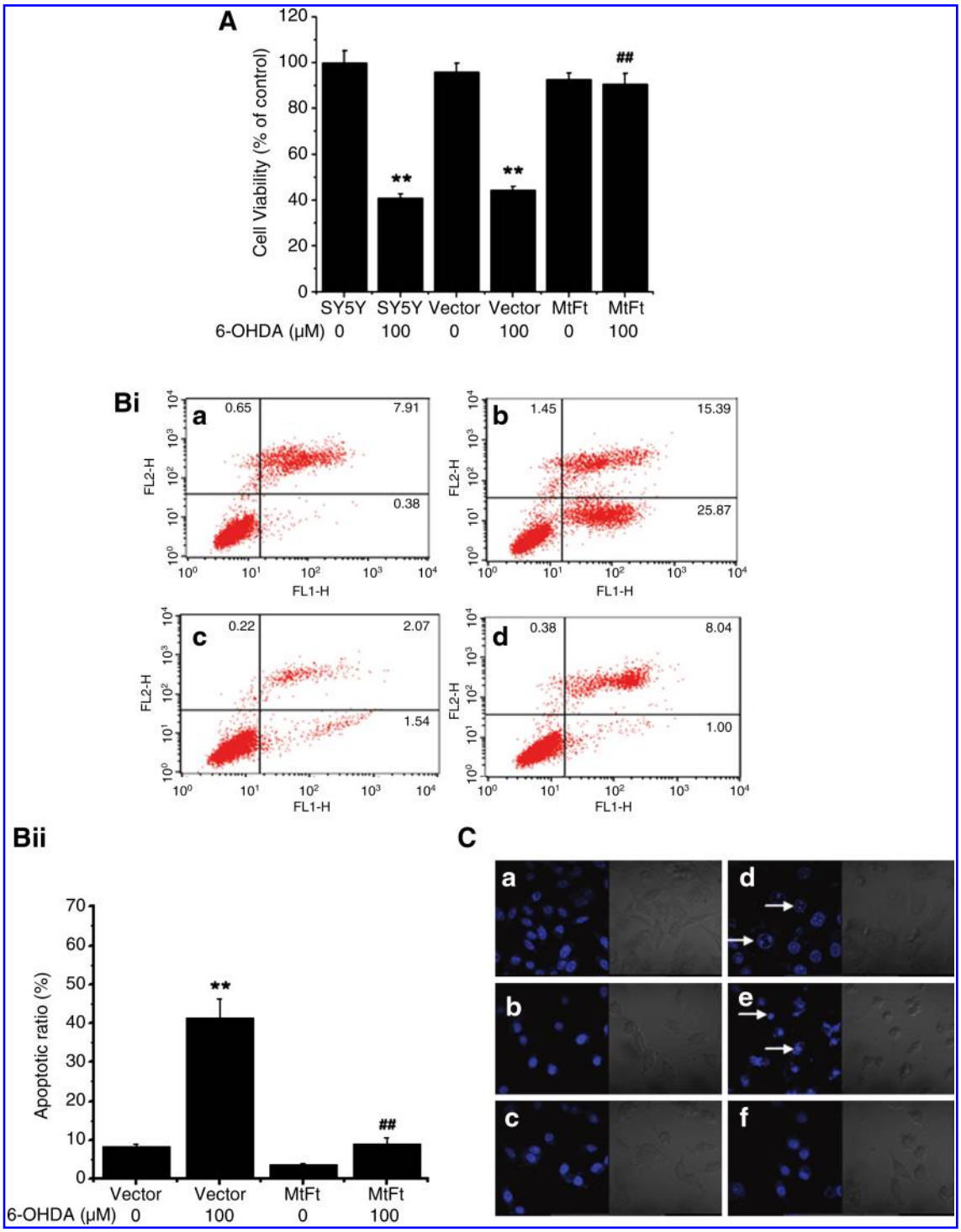

FIG. 2. Effects of MtFt expression on cell viability and apoptosis with treatment with 6-OHDA. The wild-type SH-SY5Y cells, empty vector transfectants (Vector-SY5Y), and MtFt transfectants (MtFt-SY5Y) were treated with 100 μM 6-OHDA for 24 h. (**A**) The cell viability was measured with the MTT assay. Data were expressed as percentage of the cell viability compared with untreated control cells ± SD, $n = 8$; $^{**}p < 0.01$ vs. the control cells; $^{\#\#}p < 0.01$ vs. the 6-OHDA–treated control cells. (**Bi**) Representative flow-cytometry histographs depict the protective effects of MtFt expression on 6-OHDA–induced apoptosis. (**Bii**) Statistical analysis of flow-cytometry results. Data were expressed as mean ± SD; $n = 3$. $^{**}p < 0.01$ compared with the control cells; $^{\#\#}p < 0.01$ vs. the 6-OHDA–treated control cells. (C) Micrographs of cell nuclei. The cells were stained with Hoechst 33258, and the nuclear morphology was observed with fluorescence microscopy. Nuclear size reduction, chromatin condensation, intense fluorescence, and nuclear fragmentation were considered apoptosis (arrows). (**a**) SH-SY5Y; (**b**) Vector-SY5Y; (**c**) MtFt-SY5Y; (**d**) SH-SY5Y + 6-OHDA; (**e**) Vector-SY5Y + 6-OHDA; (**f**) MtFt-SY5Y + 6-OHDA. (For interpretation of the references to color in this figure legend, the reader is referred to the web version of this article at www.liebertonline.com/ars).

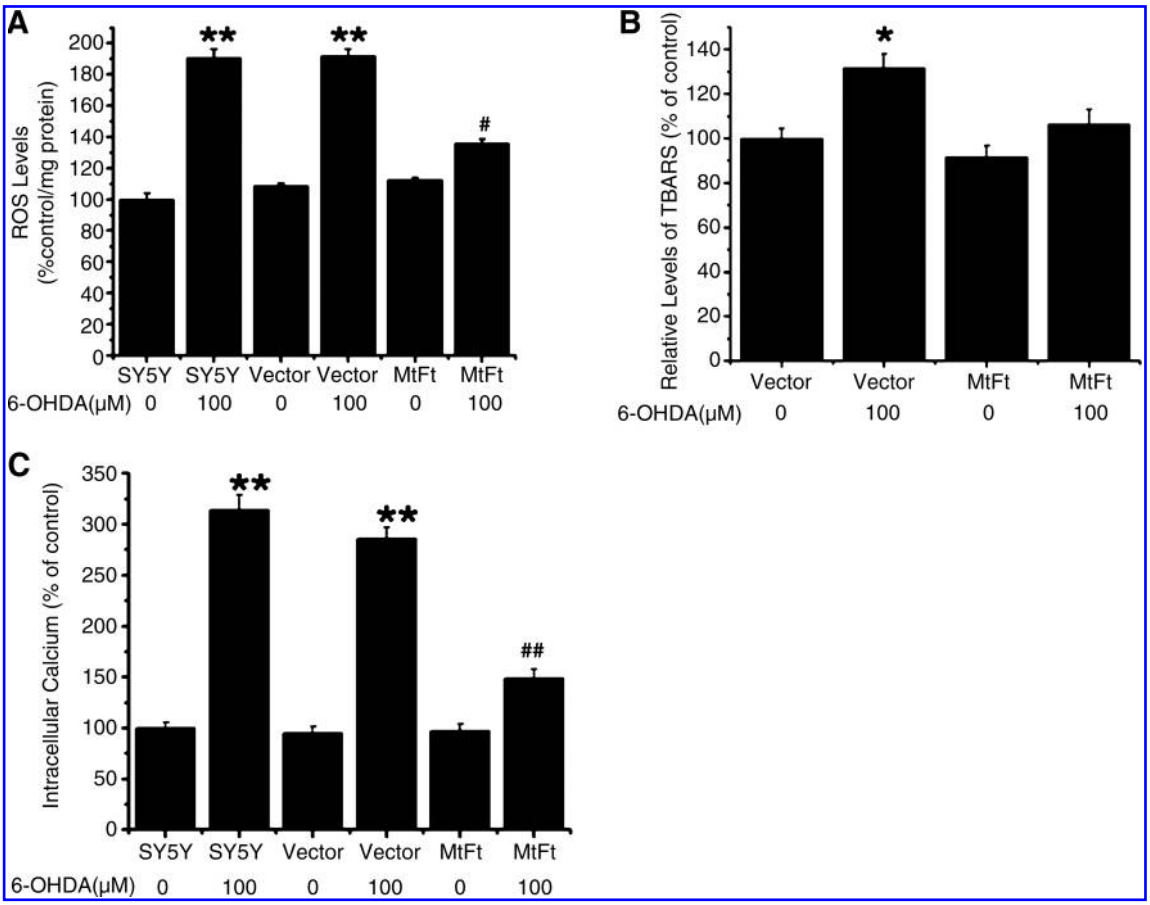

FIG. 3. MtFt expression attenuates 6-OHDA–induced accumulation of ROS (A), lipid peroxidation (TBARS) (B), and elevation of intracellular [Ca^{2+}] (C). The cells were treated with or without 100 μM 6-OHDA for 24 h, and ROS levels were detected by 2,7-dichlorofluorescein diacetate (DCF-DA) fluorescence; TBARS was measured by the absorption of TBARS at 540 nm; and the fluorescence of the $[Ca^{2+}]_i$ ion by Fluo-3AM. Data are expressed as mean ± SD, $n = 3$ (**$p < 0.01$ vs. control cells; *$p < 0.05$ vs. control cells; $^{\#\#}p < 0.01$ vs. the 6-OHDA–treated control cells; $^{\#}p < 0.05$ vs. 6-OHDA–treated control cells).

with apoptosis. It has been reported that dysfunction of mitochondria and decreased activity of complex I, II, III, and IV could induce ROS overproduction; consequently, it resulted in apoptosis (53). To examine the underlying protective mechanism of MtFt on mitochondria, the mitochondrial membrane potential (MMP) and complex I activity were measured. The results showed that 6-OHDA treatment decreased MMP by 50.79% ± 4.09% ($p < 0.01$) and 55.53% ± 5.26% ($p < 0.01$) in SH-SY5Y and Vector-SY5Y cells, respectively, compared with the control groups; however, in MtFt-SY5Y cells, the membrane potential decreased only 10.15% ± 3.45% (Fig. 4A). These results indicate that MtFt maintains the membrane potential and protects against the mitochondrial damage induced by 6-OHDA treatment.

The complex I activity reflects the stability, function, and metabolic activities of mitochondria. It has been reported that inhibition of complex I activity may induce oxidative stress and mitochondrial dysfunction (16), and 6-OHDA can inhibit complex I activity (16, 20). To determine the effects of MtFt expression on the activity of mitochondrial complex I, its activity was measured under treatment with 6-OHDA. As previously observed (17), 6-OHDA treatment decreased the complex I activity by 70% ($p < 0.01$) in Vector-SY5Y cells compared with the control groups; however, the complex I activity decreased only ~10% in MtFt-SY5Y cells (Fig. 4B). These results indicate that overexpression of MtFt protects the mitochondrial function against 6-OHDA–induced damage through preventing the loss of the activity of complex I.

Release of cytochrome *c* from mitochondria is a typical characteristic of apoptosis, which can activate a series of apoptosis cascades and lead to cell death. Figure 4C and D shows that 100 μM 6-OHDA significantly induced the release of cytochrome *c* from the mitochondria of SH-SY5Y and Vector-SY5Y cells to cytosol, indicating the cells were undergoing apoptosis; however, for MtFt-transfected cells, no significant difference was observed between 6-OHDA–treated and –untreated groups, further emphasizing that MtFt expression markedly prevents the apoptosis of SH-SY5Y cells with the treatment of 6-OHDA.

MtFt expression dramatically sustains the Bcl-2/Bax ratio and prevents caspase-3 activation

Bcl-2 and Bax are antiapoptotic and proapoptotic proteins, respectively. Our previous studies and those of others (45) reported that the Bcl-2/Bax ratio has been widely used to monitor apoptosis. When cells were treated with 6-OHDA for 24 h, the ratio of Bcl-2/Bax for Vector-SY5Y cells, quantified by Western blotting, decreased dramatically compared with

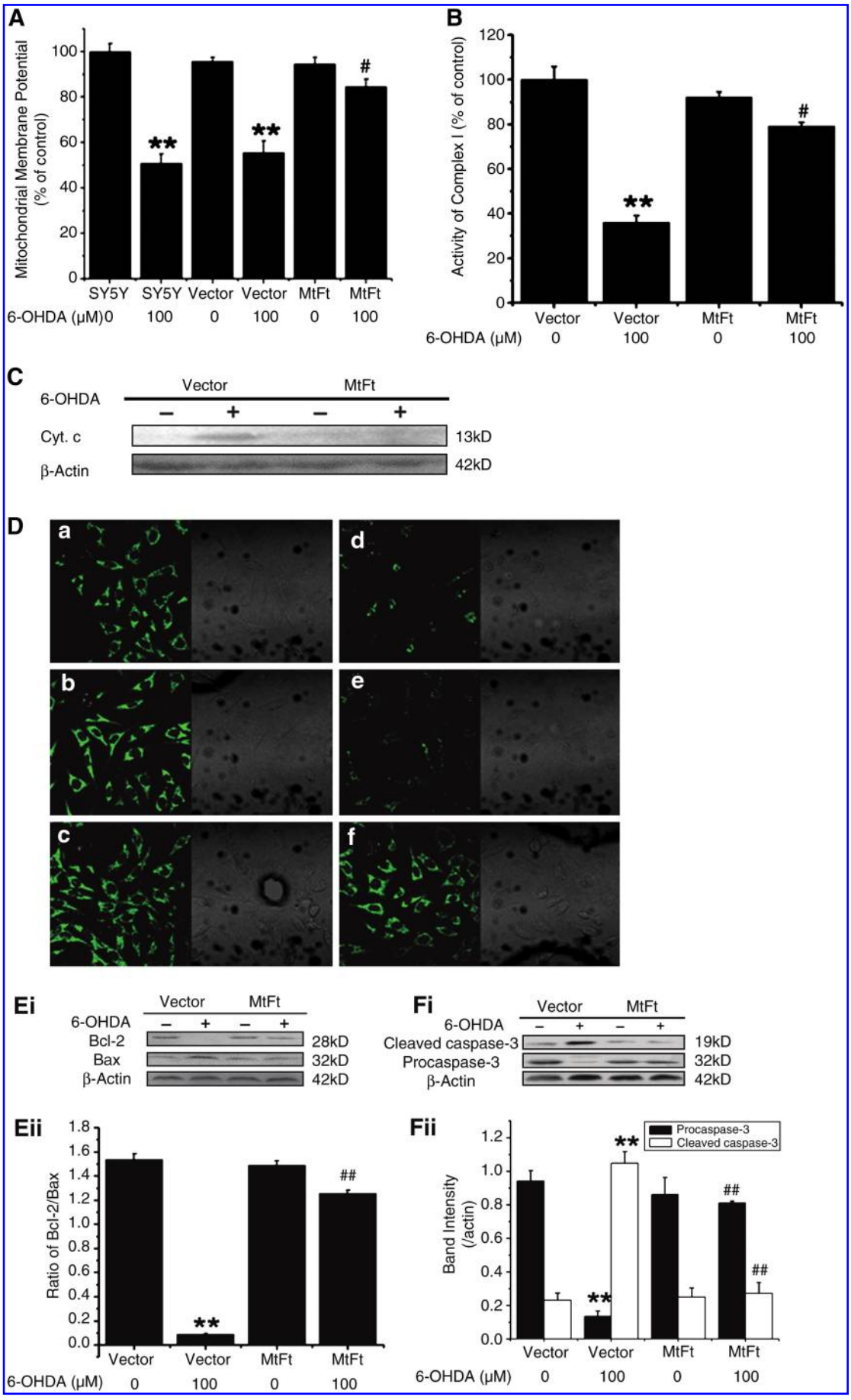
A
Mitochondrial Membrane Potential (% of control)
100
80
60
40
20
0
**
**
#
SY5Y
SY5Y
Vector
Vector
MtFt
MtFt
6-OHDA (μM) 0
100
0
100
0
100
B
Activity of Complex I (% of control)
120
100
80
60
40
20
0
**
#
Vector
Vector
MtFt
MtFt
6-OHDA (μM)
0
100
0
100
C
6-OHDA
Vector
MtFt
–
+
–
+
Cyt. c
13kD
β-Actin
42kD
D
a
d
b
e
c
f
Ei
6-OHDA
Vector
MtFt
–
+
–
+
Bcl-2
28kD
Bax
32kD
β-Actin
42kD
Fi
6-OHDA
Vector
MtFt
–
+
–
+
Cleaved caspase-3
19kD
Procaspase-3
32kD
β-Actin
42kD
Eii
Ratio of Bcl-2/Bax
1.8
1.6
1.4
1.2
1.0
0.8
0.6
0.4
0.2
0.0
**
##
Vector
Vector
MtFt
MtFt
6-OHDA (μM)
0
100
0
100
Fii
Band Intensity (/actin)
1.2
1.0
0.8
0.6
0.4
0.2
0.0
Procaspase-3
Cleaved caspase-3
**
**
##
##
Vector
Vector
MtFt
MtFt
6-OHDA (μM)
0
100
0
100

the control group; however, the ratio of Bcl-2/Bax for MtFt-SH5Y cells was not apparently changed (Fig. 4Ei and 4Eii). As shown in Fig. 4F, 6-OHDA treatment dramatically activated caspase-3 in Vector-SY5Y cells, demonstrated by an increased cleaved band of caspase-3 and a decreased band of procaspase-3; however, MtFt expression significantly prevented the procaspase-3 activation (Fig. 4Fi and 4Fii). These observations indicate that MtFt significantly maintains the normal levels of Bcl-2, decreases Bax levels, and prevents caspase-3 activation to protect the cell survival against 6-OHDA treatment.

The effects of MtFt on the levels of LIP under 6-OHDA treatment

The labile iron pool (LIP) of mammalian cells has been suggested to be the cellular free-iron source that is relatively accessible for the Fenton reaction. It has been shown (10, 30) that MtFt expression significantly mobilizes iron into mitochondria and dramatically redistributes intracellular iron levels. To measure the changes of LIP, the specific fluorescence probe calcein-AM, which binds iron specifically, and the iron chelator salicylaldehyde isonicotinoyl hydrazone (SIH) were used. As shown in Fig. 5A, only a slight, but insignificant decrease was seen in the levels of LIP in MtFt-SY5Y cells compared with Vector-SY5Y cells (columns 1 vs. 3); however, the fluorescence intensity was significantly increased by 230% in Vector-SY5Y cells after 6-OHDA treatment (columns 1 vs. 2), presumably because of rapid release of iron from various intracellular sources with the treatment with oxidants (11, 29, 44). The fluorescence signal was increased by 67% only in MtFt-SY5Y cells (Fig. 5A, columns 4 vs. 3), which is significantly lower than the changes in Vector-SY5Y cells (Fig. 5A, columns 4 vs. 2). These results indicate that the expression of MtFt slightly decreases LIP levels, but significantly blocks iron redistribution from intracellular stored iron with the treatment with 6-OHDA.

The effects of MtFt on the levels of iron proteins with 6-OHDA treatment

To clarify the mechanisms of MtFt in regulating intracellular iron homeostasis and the consequent neuroprotective roles in neuronal cells, the iron proteins involving in iron uptake, transport, and storage (Transferrin Receptor (TfR), Divalent Metal Transporter 1 (DMT1), ferroportin and H-ferritin, respectively) were studied with the treatment of 6-OHDA. First, in neuroblastoma SH-SY5Y cells, overexpression of MtFt elevated the levels of TfR (by 22%) and decreased cytosolic H-ferritin levels (by 37%; Fig. 5Bi, lane 1 vs. 3), indicating the iron deficiency of the cytoplasm, which was consistent with our previous study in H1299 lung cancer cells (30). Interestingly, when Vector-SY5Y cells were treated with 6-OHDA for 24 h, the neurotoxin significantly upregulated the levels of ferritin and downregulated the levels of TfR compared with the control groups; whereas no significant changes were found in MtFt-SY5Y cells under the same treatment (Fig. 5Bi, lane 1 vs. 2 and lane 3 vs. 4). The quantitative measurements (Fig. 5Bii) showed that 6-OHDA treatment led to <15% decrease in TfR levels in MtFt-SH5Y cells, but a 45% decrease in the vector-transfected cells; for ferritin expression, almost no change was found in MtFt-SH5Y cells, but a 25% increase in the vector-transfected cells (Fig. 5Bii). These observations are consistent with previous studies that show that oxidants treatment stimulates ferritin expression and inhibits TfR expression (29, 46). MtFt expression attenuates the changes induced by 6-OHDA treatment.

Iron-uptake experiments showed that Tf-TfR–mediated iron uptake was only slightly increased in MtFt-SH5Y cells compared with the vector-transfected counterparts (data not shown); conversely, in cancer cells, a significantly elevated iron uptake in MtFt-expressing cells was seen (30). These observations may indicate that neuronal cells have tightly controlled iron-uptake mechanism, whereas cancer cells can acquire much more iron for their fast proliferation.

To explore further other iron-transport mechanisms, DMT1 isoforms with iron-responsive elements (+IRE) and without iron-responsive elements (-IRE) and ferroportin expression were measured with Western blotting. Expression of ferroportin, the sole known iron exporter, was decreased slightly in both MtFt expression (Fig. 5Ci, lane 1 vs. 3) and 6-OHDA treatment (Fig. 5Ci, lane 1 vs. 2 and lane 3 vs. 4), indicating that iron release in those cells may be reduced. MtFt expression slightly increased DMT1 (+IRE) levels (Fig. 5Ci, lane 1 vs. 3). Interestingly, DMT1 (+IRE) levels were significantly decreased in the Vector-SY5Y cells (Fig. 5Ci, lane 1 vs. 2), but much less decrease was noted in the MtFt-SY5Y cells (Fig. 5Ci, lane 3 vs. 4) under the treatment of 6-OHDA. Furthermore, DMT1 (+IRE) levels were significantly higher in MtFt-SY5Y cells than in Vector-SH5Y cells under the treatment of 6-OHDA (Fig. 5Ci, lane 2 vs. 4). MtFt expression and 6-OHDA treatment did not affect non-IRE forms of DMT1 expression. Taken together, these results reveal that an increase in LIP in the Vector-SY5Y cells under the treatment of 6-OHDA is most likely not due to the increases in the iron uptake by TfR or DMT1, as both of these protein levels declined. The decreases in the iron exporter, ferroportin, may indicate that less iron is

FIG. 4. Overexpression of MtFt attenuates 6-OHDA–induced decreases in mitochondrial membrane potential (A), mitochondrial complex I activity (B), the release of cytochrome C from mitochondria (C, D), and effects on Bcl-2, Bax, and caspase-3 expression (E, F). The cells were treated with or without 100 μM 6-OHDA for 24 h, and the mitochondrial membrane potential was detected by the fluorescence of rhodamine 123 (**A**); complex I activity was measured as described in Materials and Methods (**B**), and cytochrome *c* was tested with Western blotting in the cytosolic fraction (**C**) and cell cytochrome c immunofluorescence in the cells (D). (**a**) SH-SY5Y; (**b**) Vector-SY5Y; (**c**) MtFt-SY5Y; (**d**) SH-SY5Y + 6-OHDA; (**e**) Vector-SY5Y + 6-OHDA; (**f**) MtFt-SY5Y + 6-OHDA. The cells were treated with or without 100 μM 6-OHDA for 24 h, and aliquots of total cell extracts were analyzed by Western blotting by using anti-Bcl-2, Bax, and β-actin (Ei) and cleaved and pro-caspase-3 (**Fi**). The ratios of Bcl-2/Bax (**Eii**) and cleaved and pro-caspase-3 (**Fii**) are shown for quantitative measurement. Data are expressed as mean ± SD, $n = 3$ ($^{**}p < 0.01$ vs. control cells; $^{*}p < 0.05$ vs. control cells; $^{\#\#}p < 0.01$ vs. the 6-OHDA–treated control cells; $^{\#}p < 0.05$ vs. 6-OHDA–treated control cells). (For interpretation of the references to color in this figure legend, the reader is referred to the web version of this article at www.liebertonline.com/ars).

released under 6-OHDA treatment and MtFt expression. The increased iron levels in LIP are most likely due to redistribution of intracellular stored and/or functional iron from various sources, such as ferritins and other iron-containing molecules (29).

The present results also show that the expression of MtFt only slightly decreased LIP levels, but dramatically inhibited the elevation of LIP levels in cells treated with 6-OHDA, presumably because of inhibiting iron redistribution from mitochondria to other cellular compartments.

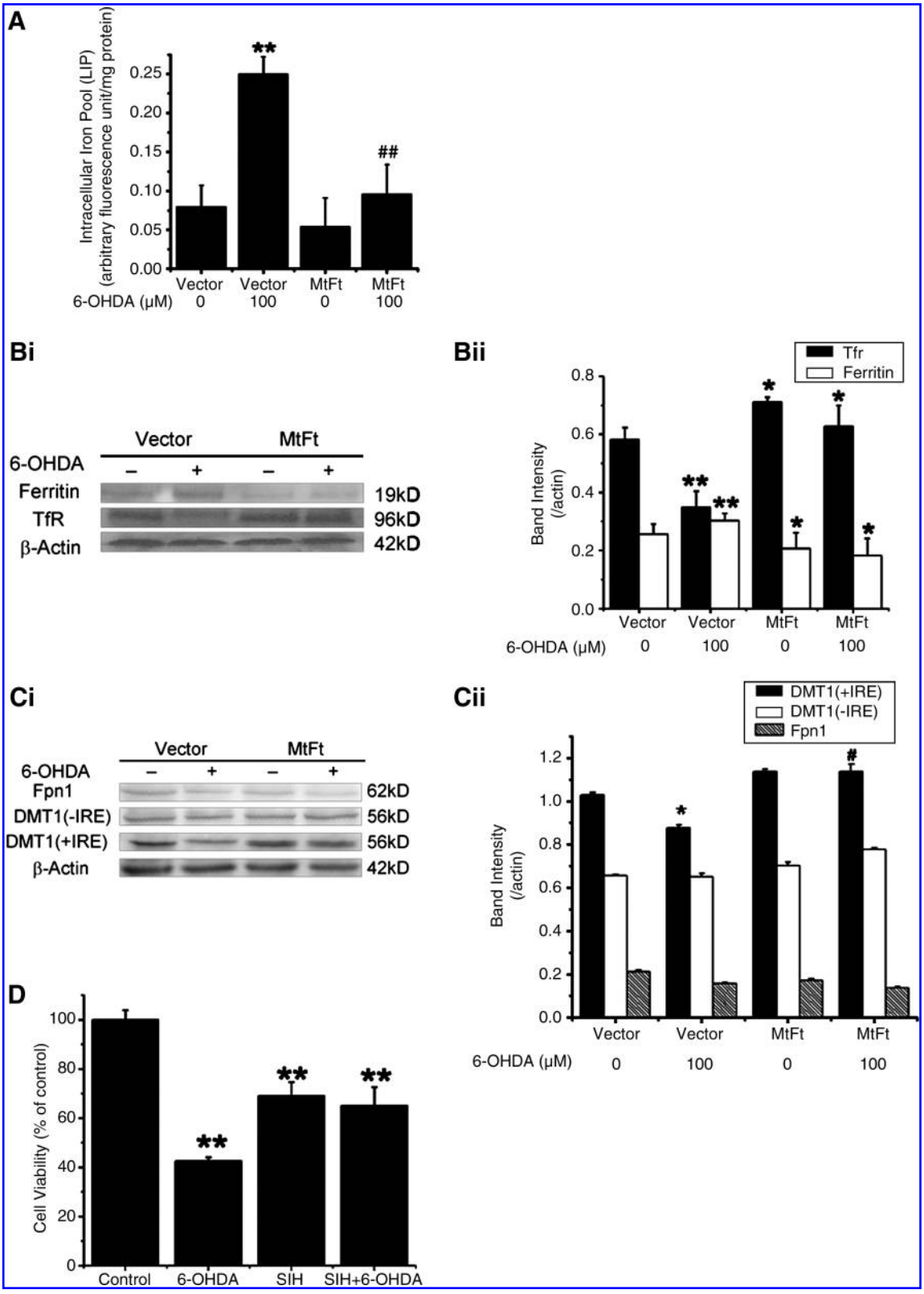

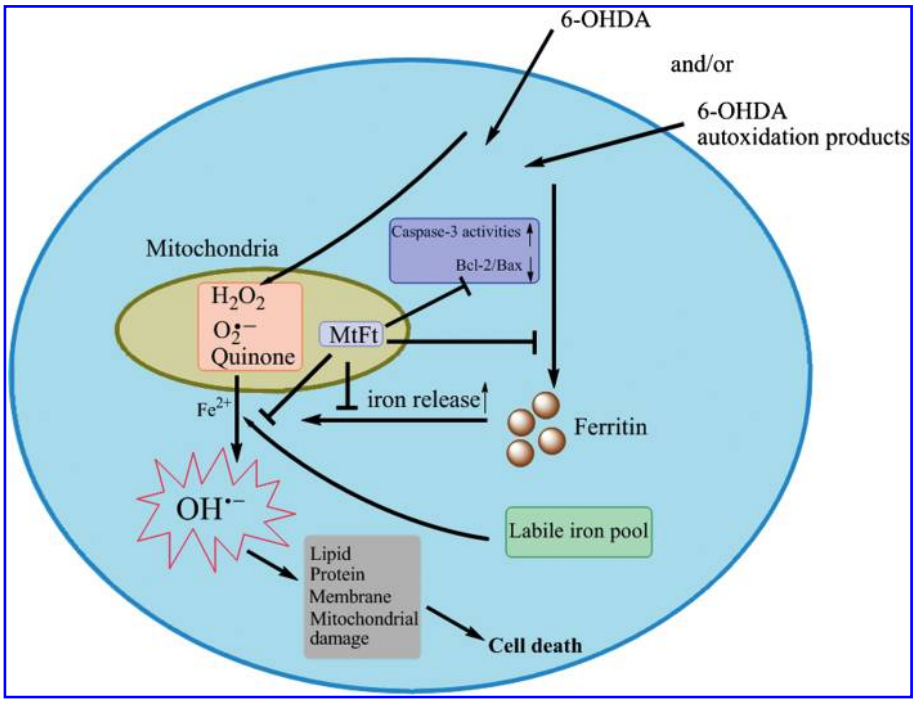

FIG. 6. A schematic representation of the proposed neuroprotective mechanism of MtFt. (For interpretation of the references to color in this figure legend, the reader is referred to the web version of this article at www.liebertonline.com/ars).

The effects of SIH on the cell viability under 6-OHDA treatment

Further to confirm that the observed neuroprotection in MtFt-SH5Y cells was due to the iron-mediated mechanism, a well-studied hydrophobic iron chelator, SIH, was used to investigate the neuroprotective roles in vector-transfected SH-SY5Y cells under treatment with 6-OHDA. 6-OHDA treatment led to a 60% decrease in cell viability. Pretreatment with the chelator significantly prevented 6-OHDA–induced loss of cell viability (60% vs. 40% cell viability; Figure 5D). The chelator treatment itself, at the current experimental concentration, also led to 40% decrease in cell viability, which reflects mainly the antiproliferation role of iron chelator SIH in limiting the iron availability for cell proliferation (36, 47, 49).

Discussion

Iron is an absolute requirement for virtually every cell, especially those of the central nervous system, which require high metabolic activity and oxygen consumption. Conversely, iron can also donate and accept electrons for the generation of ROS and can participate in the production of hydroxyl radicals through the Fenton reaction (13). Imbalance of brain iron homeostasis is considered an important contributing factor to neurotoxicity in several neurodegenerative disorders, including PD (35, 51). Accumulated evidence suggests that iron dysregulation is causative, involved in neurodegeneration, as a number of disorders of the central nervous system exhibit aberrant iron metabolism in various brain regions, as in neuroferritinopathy and Friedreich ataxia, which are associated with gene defects that encode proteins that are involved in iron storage and mitochondrial iron homeostasis (35, 51).

Ferritins are at the crossroads of iron and oxygen metabolism and have been found to protect cells significantly against oxidative stress induced by a variety of sources (3, 7, 14, 24, 32, 46). In neuronal cells, elevated ferritin expression has been shown to exert significantly neuroprotective roles in MPTP-induced experimental PD models (24). Therefore, it appears

FIG. 5. Iron homeostasis changes. (**A**)The Effects of 6-OHDA treatment on intracellular labile iron pool levels. The cells were treated with or without 100 μM 6-OHDA for 24 h. LIP was detected with the calcein-AM assay. The effects of MtFt on the expression of ferritin, TfR, DMT1 (+IRE), DMT1 (-IRE), and ferroportin1 are shown (**B, C**). The cells were treated with or without 100 μM 6-OHDA for 24 h, and aliquots of total cell extracts were analyzed with Western blotting by using anti-ferritin and anti-TfR (**Bi**), anti-DMT1(+IRE), anti-DMT1(-IRE), and anti-ferroportin1 (**Ci**). The ratios of ferritin/actin, TfR/actin (**Bii**), and DMT1 and ferroportin (**Cii**) are shown for quantitative measurement. Data are expressed as mean ± SD, $n = 3$. Data are expressed mean ± SD, $n = 3$. $^{**}p < 0.01$ vs. the control cells; $^{\#\#}p < 0.01$ vs. the MtFt-SY5Y cells. Iron chelator SIH partially prevents 6-OHDA–induced decrease in cell viability (**D**). The cells were pretreated with or without 100 μM SIH for 6 h, followed by 100 μM 6-OHDA treatment for 24 h. Cell viability was detected with the MTT assay. Data are expressed as mean ± SD, $n = 8$ ($^{**}p < 0.01$ vs. control cells; $^{*}p < 0.05$ vs. control cells; $^{\#\#}p < 0.01$ vs. the 6-OHDA–treated control cells; $^{\#}p < 0.05$ vs. 6-OHDA–treated control cells).

that neuronal cell survival is closely dependent on the cellular levels of ferritin. MtFt is a newly identified H-ferritin–like protein expressed only in mitochondria (26). The fact that the protein was identified in testis, heart, brain, spinal cord, kidney, and pancreatic islets of Langerhans but not in liver and splenocytes under physiologic conditions indicates that the major role of MtFt may be to protect mitochondria from iron-dependent oxidative damage in cells characterized by high metabolic activity and oxygen consumption (38). MtFt expression also prevented, at least in part, oxidative stress–induced damage of frataxin-defective yeast and HeLa cells (6, 7). However, no reports are available on its roles in the nervous system.

In the current study, MtFt was shown to have a specific expression pattern in different brain regions, and its levels altered on iron-metabolism dysregulation in *Ireb2*$^{-/-}$ mice. Our results showed a prominent downregulation of MtFt in the cerebellum and but not in the striatum of *Ireb2*$^{-/-}$ mice, which produced iron accumulation in the brain and developed progressive PD-like neurodegeneration. In the cerebellum of *Ireb2*$^{-/-}$ mice, severe Purkinje cell loss and ultrastructural evidence of degeneration were detected in many of the remaining Purkinje cells. Abnormal elevation of cytosolic ferritin colocalizing with iron accumulations in populations of neurons that degenerate is the most striking feature in these mice: both L- and H-ferritin significantly increased in cerebellum and striatum in the *Ireb2*$^{-/-}$ mice compared with the wild-type animals (25, 39). Therefore, it was tempting to speculate that the altered expression of MtFt may associate with the neurodegeneration in the cerebellum of *Ireb2*$^{-/-}$mice, which have a profound dysregulation of neuronal iron metabolism that may be potentially important in pathophysiologic events, such as in PD. To elucidate the relation of MtFt expression and neuronal cell death observed in IRP2-knockout mice and an experimental PD model induced by neurotoxin 6-OHDA, we studied the roles of MtFt on iron metabolism and cell susceptibility to the neurotoxin in dopaminergic neuroblastoma SH-SY5Y cells.

To assess how MtFt overexpression affects the response of cells to 6-OHDA, stable expression of MtFt in SH-SY5Y cells was established to elucidate the roles of MtFt expression in the neuroblastoma cells subjected to oxidative stress. We demonstrate here that overexpression of MtFt significantly protected SH-SY5Y cells against 6-OHDA–induced and oxidative stress–mediated apoptosis (Figs. 2–4). It has been reported that the autooxidation and enzymatic oxidation of dopamine lead to the generation of ROS, which is speculated to be one of the contributing factors of PD pathogenesis (5, 41). Our study shows that the neuroprotective effects of MtFt are dependent on ROS-mediated pathways. MtFt expression diminishes overproduction of ROS and lipid peroxidation and represses the loss of MMP (Figs. 2–4). ROS also are generated from the dysfunction of the mitochondrial respiratory chain, such as inhibition of complex I activity (21). Our results showed that MtFt expression protects against the loss of complex I activity and mitochondrial protein cytochrome *c* release from the organelle. Taken together, these observations demonstrate that regulating mitochondrial iron availability by the expression of MtFt is a powerful way to diminish oxidative stress–mediated cell damage.

Bcl-2 and Bax play important roles in the oxidative stress–mediated neuronal cell apoptosis (28, 33). It was reported that Bcl-2 protected neurons against oxidant stress and apoptosis in PD (45). Bcl-2 also maintained the mitochondrial integrity by blocking the release of apoptogenic factors such as cytochrome *c* from mitochondria into cytoplasm. Our results showed that MtFt can increase the Bcl-2 levels and prevent caspase-3 activation and, as a result, promote cell survival (Fig. 4E and F).

It is still controversial whether iron is a causal factor in PD or a consequence of neuronal degeneration (1, 4, 43). Our current study, to the best of our knowledge, is the first to demonstrate the potential correlation between ferritin expressed in mitochondria and neuroprotective effects. MtFt expression in dopaminergic neuroblastoma cells can markedly regulate intracellular iron metabolism. As shown in Fig. 5B and C, MtFt expression induced an iron-deficiency phenotype in the cells, and this iron depletion significantly abrogated 6-OHDA–induced increases in the LIP levels. Western blotting of iron protein expression further demonstrated that the increased LIP under the treatment of 6-OHDA was not due to increased iron uptake or decreased iron release, as TfR, DMT1 (+IRE), and ferroportin levels decreased on 6-OHDA treatment. Instead, intracellular iron redistribution may account for the increased levels of LIP, especially iron released from cytosolic ferritins (29). 6-OHDA has been reported to be able to release iron from ferritin storage (22, 41), and the released iron may catalyze a Fenton reaction; consequently, damage of mitochondria and induction of cell death occur.

To determine the involvement of iron in mediating cell damage by 6-OHDA, we investigated the relation between the iron chelator SIH and the prevention of cell damage. It has been shown that SIH also significantly prevented 6-OHDA–induced cell damage (Fig. 5D), which is consistent with our previous observations that DFO and SIH could prevent *tert*-butyl hydroperoxide–mediated cell damage (29).

Although previous studies have shown that MtFt overexpression markedly affects intracellular iron homeostasis and restores defects caused by frataxin deficiency (6, 7, 50), the physiologic function of MtFt is still elusive. The current study demonstrates a close relation between MtFt expression and prevention of neuronal cell degeneration in both IRP2 knockout mice and 6-OHDA–induced SH-SY5Y cells. The schematic representation of the proposed mechanism delineated in this study has been summarized in Fig. 6. More important, MtFt significantly protects 6-OHDA–induced neuroblastoma cell damage through redox signal pathways, which are coordinately regulated by intracellular iron levels. Moreover, the current study also suggests that chelation of mitochondrial iron may be a feasible way to prevent neurotoxicity, as mitochondria play essential role in oxidative stress–mediated cell damage. Because no IRE structure exists in the *MtFt* gene, the expression of MtFt may not be regulated by the IRE/IRP system, as seen in cytosolic ferritin and TfR. Further study should focus on the mechanism of regulation of MtFt expression in neuronal cells.

In summary, the current study for the first time demonstrates the role of MtFt in neuroprotection. Appropriate regulation of MtFt expression may prevent the damage to neuronal cells induced by neurotoxin and in the pathologic conditions observed in patients with PD. Mitochondrial iron chelation provides a new neuroprotective strategy for PD.

Acknowledgments

This work was supported by grants from the National Natural Sciences Foundation of China (30871260; 10979011; 30900278), Natural Science Foundation of Hebei Province (C2007000251), High Technology Research and Development Project of China (2009AA03Z335) and the State Key Development Program for Basic Research of China (2010CB933600). GN gratefully acknowledges the support of Chinese Academy of Sciences, Hundred Talents Program. We also thank Dr. Manik Ghosh and Hayden Ollivierre-Wilson for preparation of the IRP-knockout mouse. Anti-MtFt antibody was a generous gift from Professor Sonia Levi and Dr. Paolo Santambrogio, Milan.

Author Disclosure Statement

The authors declare no competing financial interests.

References

1. Adams JD Jr and Odunze IN. Oxygen free radicals and Parkinson's disease. *Free Radic Biol Med* 10: 161–269, 1991.
2. Arosio P, Ingrassia R, and Cavadini P. Ferritins: a family of molecules for iron storage, antioxidation and more. *Biochim Biophys Acta* 1790: 589–599, 2009.
3. Arosio P and Levi S. Ferritin, iron homeostasis, and oxidative damage. *Free Radic Biol Med* 33: 457–463, 2002.
4. Berg D, Gerlach M, Youdim MB, Double KL, Zecca L, Riederer P, and Becker G. Brain iron pathways and their relevance to Parkinson's disease. *J Neurochem* 79: 225–236, 2001.
5. Bove J, Prou D, Perier C, and Przedborski S. Toxin-induced models of Parkinson's disease. *NeuroRx* 2: 484–494, 2005.
6. Campanella A, Isaya G, O'Neill HA, Santambrogio P, Cozzi A, Arosio P, and Levi S. The expression of human mitochondrial ferritin rescues respiratory function in frataxin-deficient yeast. *Hum Mol Genet* 13: 2279–2288, 2004.
7. Campanella A, Rovelli E, Santambrogio P, Cozzi A, Taroni F, and Levi S. Mitochondrial ferritin limits oxidative damage regulating mitochondrial iron availability: hypothesis for a protective role in Friedreich ataxia. *Hum Mol Genet* 18: 1–11, 2009.
8. Campos CB, Paim BA, Cosso RG, Castilho RF, Rottenberg H, and Vercesi AE. Method for monitoring of mitochondrial cytochrome c release during cell death: immunodetection of cytochrome c by flow cytometry after selective permeabilization of the plasma membrane. *Cytometry A* 69: 515–523, 2006.
9. Cohen G. Oxy-radical toxicity in catecholamine neurons. *Neurotoxicology* 5: 77–82, 1984.
10. Corsi B, Cozzi A, Arosio P, Drysdale J, Santambrogio P, Campanella A, Biasiotto G, Albertini A, and Levi S. Human mitochondrial ferritin expressed in HeLa cells incorporates iron and affects cellular iron metabolism. *J Biol Chem* 277: 22430–22437, 2002.
11. Deb S, Johnson EE, Robalinho-Teixeira RL, and Wessling-Resnick M. Modulation of intracellular iron levels by oxidative stress implicates a novel role for iron in signal transduction. *Biometals* 22: 855–862, 2009.
12. Dexter DT, Wells FR, Agid F, Agid Y, Lees AJ, Jenner P, and Marsden CD. Increased nigral iron content in postmortem parkinsonian brain. *Lancet* 2: 1219–1220, 1987.
13. Eaton JW and Qian M. Molecular bases of cellular iron toxicity. *Free Radic Biol Med* 32: 833–840, 2002.
14. Epsztejn S, Kakhlon O, Glickstein H, Breuer W, and Cabantchik I. Fluorescence analysis of the labile iron pool of mammalian cells. *Anal Biochem* 248: 31–40, 1997.
15. Gee P and Davison AJ. Intermediates in the aerobic autoxidation of 6-hydroxydopamine: relative importance under different reaction conditions. *Free Radic Biol Med* 6: 271–284, 1989.
16. Glinka YY and Youdim MB. Inhibition of mitochondrial complexes I and IV by 6-hydroxydopamine. *Eur J Pharmacol* 292: 329–332, 1995.
17. Guo S, Bezard E, and Zhao B. Protective effect of green tea polyphenols on the SH-SY5Y cells against 6-OHDA induced apoptosis through ROS-NO pathway. *Free Radic Biol Med* 39: 682–695, 2005.
18. Guo S, Yan J, Yang T, Yang X, Bezard E, and Zhao B. Protective effects of green tea polyphenols in the 6-OHDA rat model of Parkinson's disease through inhibition of ROS-NO pathway. *Biol Psychiatry* 62: 1353–1362, 2007.
19. Halliwell B. Reactive oxygen species and the central nervous system. *J Neurochem* 59: 1609–1623, 1992.
20. Harley A, Cooper JM, and Schapira AH. Iron induced oxidative stress and mitochondrial dysfunction: relevance to Parkinson's disease. *Brain Res* 627: 349–353, 1993.
21. He Y, Leung KW, Zhang YH, Duan S, Zhong XF, Jiang RZ, Peng Z, Tombran-Tink J, and Ge J. Mitochondrial complex I defect induces ROS release and degeneration in trabecular meshwork cells of POAG patients: protection by antioxidants. *Invest Ophthalmol Vis Sci* 49: 1447–1458, 2008.
22. Jameson GN, Jameson RF, and Linert W. New insights into iron release from ferritin: direct observation of the neurotoxin 6-hydroxydopamine entering ferritin and reaching redox equilibrium with the iron core. *Org Biomol Chem* 2: 2346–2351, 2004.
23. Janssen AJ, Trijbels FJ, Sengers RC, Smeitink JA, van den Heuvel LP, Wintjes LT, Stoltenborg-Hogenkamp BJ, and Rodenburg RJ. Spectrophotometric assay for complex I of the respiratory chain in tissue samples and cultured fibroblasts. *Clin Chem* 53: 729–734, 2007.
24. Kaur D, Yantiri F, Rajagopalan S, Kumar J, Mo JQ, Boonplueang R, Viswanath V, Jacobs R, Yang L, Beal MF, DiMonte D, Volitaskis I, Ellerby L, Cherny RA, Bush AI, and Andersen JK. Genetic or pharmacological iron chelation prevents MPTP-induced neurotoxicity in vivo: a novel therapy for Parkinson's disease. *Neuron* 37: 899–909, 2003.
25. LaVaute T, Smith S, Cooperman S, Iwai K, Land W, Meyron-Holtz E, Drake SK, Miller G, Abu-Asab M, Tsokos M, Switzer R, 3rd, Grinberg A, Love P, Tresser N, and Rouault TA. Targeted deletion of the gene encoding iron regulatory protein-2 causes misregulation of iron metabolism and neurodegenerative disease in mice. *Nat Genet* 27: 209–214, 2001.
26. Levi S, Corsi B, Bosisio M, Invernizzi R, Volz A, Sanford D, Arosio P, and Drysdale J. A human mitochondrial ferritin encoded by an intronless gene. *J Biol Chem* 276: 24437–24440, 2001.
27. Lin MT and Beal MF. Mitochondrial dysfunction and oxidative stress in neurodegenerative diseases. *Nature* 443: 787–795, 2006.
28. Lipton SA. Janus faces of NF-kappa B: neurodestruction versus neuroprotection. *Nat Med* 3: 20–22, 1997.
29. Lu ZB, Nie GJ, Li YY, Soe-Lin S, Tao Y, Cao YL, Zhang ZY, Liu NQ, Ponka P, and Zhao BL. Overexpression of mitochondrial ferritin sensitizes cells to oxidative stress via an iron-mediated mechanism. *Antioxid Redox Signal* 11: 1791–1803, 2009.

30. Nie G, Sheftel AD, Kim SF, and Ponka P. Overexpression of mitochondrial ferritin causes cytosolic iron depletion and changes cellular iron homeostasis. *Blood* 105: 2161–2167, 2005.
31. Oh YM, Jang EH, Ko JH, Kang JH, Park CS, Han SB, Kim JS, Kim KH, Pie JE, and Shin DW. Inhibition of 6-hydroxydopamine-induced endoplasmic reticulum stress by l-carnosine in SH-SY5Y cells. *Neurosci Lett* 459: 7–10, 2009.
32. Omiya S, Hikoso S, Imanishi Y, Saito A, Yamaguchi O, Takeda T, Mizote I, Oka T, Taneike M, Nakano Y, Matsumura Y, Nishida K, Sawa Y, Hori M, and Otsu K. Downregulation of ferritin heavy chain increases labile iron pool, oxidative stress and cell death in cardiomyocytes. *J Mol Cell Cardiol* 46: 59–66, 2009.
33. Oshima Y, Akiyama T, Hikita A, Iwasawa M, Nagase Y, Nakamura M, Wakeyama H, Kawamura N, Ikeda T, Chung UI, Hennighausen L, Kawaguchi H, Nakamura K, and Tanaka S. Pivotal role of Bcl-2 family proteins in the regulation of chondrocyte apoptosis. *J Biol Chem* 283: 26499–26508, 2008.
34. Parkinson J. An essay on the shaking palsy, 1817. *J Neuropsychiatry Clin Neurosci* 14: 223–236, 2002.
35. Ponka P. Hereditary causes of disturbed iron homeostasis in the central nervous system. *Ann NY Acad Sci* 1012: 267–281, 2004.
36. Richardson DR. Iron chelators as therapeutic agents for the treatment of cancer. *Crit Rev Oncol Hematol* 42: 267–281, 2002.
37. Ryu EJ, Harding HP, Angelastro JM, Vitolo OV, Ron D, and Greene LA. Endoplasmic reticulum stress and the unfolded protein response in cellular models of Parkinson's disease. *J Neurosci* 22: 10690–10698, 2002.
38. Santambrogio P, Biasiotto G, Sanvito F, Olivieri S, Arosio P, and Levi S. Mitochondrial ferritin expression in adult mouse tissues. *J Histochem Cytochem* 55: 1129–1137, 2007.
39. Smith SR, Cooperman S, Lavaute T, Tresser N, Ghosh M, Meyron-Holtz E, Land W, Ollivierre H, Jortner B, Switzer R 3rd, Messing A, and Rouault TA. Severity of neurodegeneration correlates with compromise of iron metabolism in mice with iron regulatory protein deficiencies. *Ann N Y Acad Sci* 1012: 65–83, 2004.
40. Sofic E, Riederer P, Heinsen H, Beckmann H, Reynolds GP, Hebenstreit G, and Youdim MB. Increased iron (III) and total iron content in post mortem substantia nigra of parkinsonian brain. *J Neural Transmission* 74: 199–205, 1988.
41. Soto-Otero R, Mendez-Alvarez E, Hermida-Ameijeiras A, Munoz-Patino AM, and Labandeira-Garcia JL. Autoxidation and neurotoxicity of 6-hydroxydopamine in the presence of some antioxidants: potential implication in relation to the pathogenesis of Parkinson's disease. *J Neurochem* 74: 1605–1612, 2000.
42. Storch A, Kaftan A, Burkhardt K, and Schwarz J. 6-Hydroxydopamine toxicity towards human SH-SY5Y dopaminergic neuroblastoma cells: independent of mitochondrial energy metabolism. *J Neural Transmission* 107: 281–293, 2000.
43. Thompson KJ, Shoham S, and Connor JR. Iron and neurodegenerative disorders. *Brain Res Bull* 55: 155–164, 2001.
44. Torti FM and Torti SV. Regulation of ferritin genes and protein. *Blood* 99: 3505–3516, 2002.
45. Tortosa A, Lopez E, and Ferrer I. Bcl-2 and Bax proteins in Lewy bodies from patients with Parkinson's disease and diffuse Lewy body disease. *Neurosci Lett* 238: 78–80, 1997.
46. Tsuji Y, Ayaki H, Whitman SP, Morrow CS, Torti SV, and Torti FM. Coordinate transcriptional and translational regulation of ferritin in response to oxidative stress. *Mol Cell Biol* 20: 5818–5827, 2000.
47. Whitnall M, Howard J, Ponka P, and Richardson DR. A class of iron chelators with a wide spectrum of potent antitumor activity that overcomes resistance to chemotherapeutics. *Proc Natl Acad Sci U S A* 103: 14901–14906, 2006.
48. Yamamuro A, Yoshioka Y, Ogita K, and Maeda S. Involvement of endoplasmic reticulum stress on the cell death induced by 6-hydroxydopamine in human neuroblastoma SH-SY5Y cells. *Neurochem Res* 31: 657–664, 2006.
49. Yuan J, Lovejoy DB, and Richardson DR. Novel di-2-pyridyl-derived iron chelators with marked and selective antitumor activity: in vitro and in vivo assessment. *Blood* 104: 1450–1458, 2004.
50. Zanella I, Derosas M, Corrado M, Cocco E, Cavadini P, Biasiotto G, Poli M, Verardi R, and Arosio P. The effects of frataxin silencing in HeLa cells are rescued by the expression of human mitochondrial ferritin. *Biochim Biophys Acta* 1782: 90–98, 2008.
51. Zecca L, Youdim MB, Riederer P, Connor JR, and Crichton RR. Iron, brain ageing and neurodegenerative disorders. *Nat Rev Neurosci* 5: 863–873, 2004.
52. Zhang Y, Dawson VL, and Dawson TM. Oxidative stress and genetics in the pathogenesis of Parkinson's disease. *Neurobiol Dis* 7: 240–250, 2000.
53. Zhang Y and Zhao B. Green tea polyphenols enhance sodium nitroprusside-induced neurotoxicity in human neuroblastoma SH-SY5Y cells. *J Neurochem* 86: 1189–1200, 2003.

Address correspondence to:
Prof. Yan-Zhong Chang
Laboratory of Molecular Iron Metabolism
College of Life Science
Hebei Normal University
Shijiazhuang, 050016, Hebei Province
China

E-mail: frankyzchang@yahoo.com.hk

or

Prof. Bao-Lu Zhao
State Key Laboratory of Brain and Cognitive Science
Institute of Biophysics
Chinese Academy of Sciences
Beijing, 100101
China

E-mail: zhaobl@sun5.ibp.ac.cn

Date of first submission to ARS Central, November 22, 2009; date of final revised submission, January 12, 2010; date of acceptance, January 31, 2010.

Abbreviations Used

6-OHDA = 6-hydrodopamine
IRPs = iron-regulatory proteins (IRPs)
MtFt = mitochondrial ferritin
PD = Parkinson's disease
ROS = reactive oxygen species

This article has been cited by:

1. Wen-Shuang Wu , Ya-Shuo Zhao , Zhen-Hua Shi , Shi-Yang Chang , Guang-Jun Nie , Xiang-Lin Duan , Song-Min Zhao , Qiong Wu , Zhen-Ling Yang , Bao-Lu Zhao , Yan-Zhong Chang . Mitochondrial Ferritin Attenuates #-Amyloid-Induced Neurotoxicity: Reduction in Oxidative Damage Through the Erk/P38 Mitogen-Activated Protein Kinase Pathways. *Antioxidants & Redox Signaling*, ahead of print. [Abstract] [Full Text HTML] [Full Text PDF] [Full Text PDF with Links] [Supplemental material]
2. Andrzej Friedman, Paolo Arosio, Dario Finazzi, Dariusz Koziorowski, Jolanta Galazka-Friedman. 2011. Ferritin as an important player in neurodegeneration. *Parkinsonism & Related Disorders* **17**:6, 423-430. [CrossRef]
3. Gabriela A. Salvador, Romina M. Uranga, Norma M. Giusto. 2011. Iron and Mechanisms of Neurotoxicity. *International Journal of Alzheimer's Disease* **2011**, 1-9. [CrossRef]
4. Li Wan, Guangjun Nie, Jie Zhang, Yunfeng Luo, Peng Zhang, Zhiyong Zhang, Baolu Zhao. 2011. #-Amyloid peptide increases levels of iron content and oxidative stress in human cell and Caenorhabditis elegans models of Alzheimer disease. *Free Radical Biology and Medicine* **50**:1, 122-129. [CrossRef]